Published in final edited form as:
J Am Chem Soc. 2012 January 11; 134(1): 130–133. doi:10.1021/ja209533x.

Second-Chance Forward Isomerization Dynamics of the Red/Green Cyanobacteriochrome NpR6012g4 from *Nostoc punctiforme*

Peter W. Kim[1], **Lucy H. Freer**[1], **Nathan C. Rockwell**[2], **Shelley S. Martin**[2], **J. Clark Lagarias**[2], and **Delmar S. Larsen**[1,*]

[1]Department of Chemistry, University of California, One Shields Avenue, Davis, CA 95616

[2]Department of Molecular and Cell Biology, University of California, One Shields Avenue, Davis, CA 95616

Abstract

The primary ultrafast Z-to-E isomerization photodynamics of the phytochrome-related cyanobacteriochrome (CBCR) NpR6012g4 from *N. punctiforme* were studied by transient absorption pump-dump-probe spectroscopy. A 2-ps dump pulse resonant with the stimulated emission band depleted 21 % of the excited-state population, while the initial photoproduct Lumi-R was depleted by only 11 %. We observe a red-shifted ground-state intermediate (GSI) that we assign to a metastable state that failed to fully isomerize. Multi-component global analysis implicates the generation of additional Lumi-R from GSI via crossing over the ground-state thermal barrier for full isomerization, explaining the discrepancy of excited-state and Lumi-R depletion by the dump pulse. This *second-chance* ground-state dynamics provides a plausible explanation for the unusually high quantum yield of 40 % for the primary isomerization step in the forward reaction of NpR6012g4.

Keywords

photoreceptors; transient absorption spectroscopy; cyanobacteriochrome; phytochromes; quantum yield; pump-dump-probe

Phytochromes are bilin chromophore-based photoswitching proteins first discovered in plants and later in bacteria and fungi.[1-2] Phytochromes modulate various physiological responses, including shade avoidance in plants, and photoconvert between red (~660 nm, P_r) and far-red (~720 nm, P_{fr}) absorbing states.[3] Phytochromes share a bilin-binding GAF (cGMP phosphodiesterase/adenylyl cyclase/FhlA) domain with the distantly related cyanobacteriochromes (CBCRs).[4] While phytochromes typically require one or more flanking domains for stability, photo-conversion, and bilin binding, the CBCR GAF domain is sufficient to bind the phycocyanobilin (PCB) chromophore (Fig. 1) and trigger photoresponses encompassing the entire spectral region from ultraviolet to red.[4-6] CBCRs are small (< 200 residues) and exhibit broad spectral sensitivity; moreover, they can readily be expressed in *E. coli* cells engineered for bilin biosynthesis.[7] CBCRs are therefore attractive systems for study of protein-chromophore interactions and ultrafast photochemical dynamics as well as for development of fluorescent or optogenetic probes.[8-11]

*Corresponding author: dlarsen@ucdavis.edu.

Supporting Information Available: Experimental procedures and supplementary results are available free of charge via the Internet at http://pubs.acs.org.

For the extended family of phytochrome photosensors, it is generally accepted that light triggers the Z to E isomerization of the bilin C15,16 double bond, which leads to rotation of the D-ring (Fig. 1).[5] The photoisomerization quantum yield (Φ) for canonical phytochromes has been estimated to be 10-15 %,[12-13] significantly lower than that of other isomerizing photoreceptors such as rhodopsin (Φ = 65 %) or the photoactive yellow protein (Φ = 35%).[14-15] Recently from ultrafast visible pump-probe (PP) spectroscopy, we reported that the red/green CBCR NpR6012g4 from *Nostoc punctiforme* ATCC 29133 exhibits a photoisomerization Φ of 32% in the forward (red-to-green or P_r-to-P_g) direction.[16] This is the highest yield so far reported for any phytochrome-based sensor system. Here, we explore the primary initiation dynamics underlying this unusually high Φ with femtosecond dispersed pump-dump-probe (PDP) spectroscopy.

Understanding how quantum yields are modulated in photoactive systems is of significant importance in designing novel optogenetic tools and *in vivo* fluorescence markers.[8-9,11] Ultrafast visible PP spectroscopy, though widely successful in studying the photodynamics of many photoactive proteins,[17-20] has limitations for studying for forward dynamics of NpR6012g4 ($P_r \rightarrow P_r^* \rightarrow$ Lumi-R $\rightarrow P_g$) due to the significant spectral and temporal overlap between the excited-state (P_r^*) and ground-state absorptions of P_r and the primary photoproduct Lumi-R. Furthermore, PP signals are largely insensitive to timescales in which fast intermediates form after slower dynamics. Multipulse broadband PDP signals circumvent these limitations, providing greater insight into the primary photo-induced dynamics, while resolving underlying dynamics and populations that were not accessible with PP experiments alone.[21-23] In the PDP experiment, a ‘pump’ pulse excites the ground state population and a second ‘dump’ pulse de-excites the excited-state population after a defined delay time. As demonstrated here, the dump pulse should be selected to be spectrally and temporally resonant with the stimulated emission (SE) band alone so that only the excited-state population is depleted. Consequently, photoproducts that would be derived from the dumped excited-state population are subsequently depleted.

Figure 2A shows the pump and dump pulses overlaid on the ground-state absorption and fluorescence emission bands of P_r in NpR6012g4. PP transient spectra at various probe times are depicted in Figure 2B. The 2-ps to 100-ps spectra clearly show excited-state features of P_r^*, including a positive excited-state absorption (ESA) band (440 - 580 nm) and a broad negative SE band (> 680 nm). On longer timescales (>1 ns), the transient spectra exhibit a positive absorption at 675 nm with a bleach (loss of ground-state absorption) at 650 nm, indicating formation of the Lumi-R photoproduct (magenta curve).[16] The 740-nm dump pulse is applied 2 ps after the pump pulse and is selectively resonant with the SE band of P_r^* (Fig. 2B, black curve), allowing partial de-excitation of the P_r^* population.

Figure 3 contrasts the PP (black circles) and PDP (red circles) signals at selected probe wavelengths. Dump-induced depletion of the excited state is observed as an instantaneous and persistent loss of both ESA (470 nm) and SE (680 and 737 nm) bands. However, at 597 nm, where the PP signal is initially zero (due to overlap of ESA and bleach), the dump-induced depletion of the ESA signal results in a negative signal that rapidly decays on a 10-ps timescale (Fig. 3B). This tracks the kinetics of the ground-state population and is not observed in PP signals alone.[16]

The PDP kinetics can be resolved spectrally at various probe times (Figure 4). The constructed ΔΔOD signals represent the dump-induced dynamics of the PP signals and are calculated as PDP–PP–DP, where DP is the dump-probe trace. While DP contains no photoinduced signals (Fig. S1), it does contain artifactual cross-phase modulation signals that are (mostly) absent in the ΔΔOD signals.[24] To remove the depletion of P_r^* from the ΔΔOD signal and resolved only the dump-induced ground-state dynamics, we subtracted

scaled PP signals from the PDP signals after normalizing the two signals to the ESA in the PP signal from 440—520 nm (Fig. 2B), which is only sensitive to the P_r* population. These excited-state-normalized-spectra (ESNS) signals track only the ground-state kinetics and assuming the P_r* spectrum does not change in time, which we previously established for NpR6012g4.[16]

The 2.6-ps ESNS, calculated 600-fs after the dumping, exhibits a positive absorption band peaking around 680 nm (Fig. 4A green) that we attribute to a GSI. GSIs have been observed in other PDP experiments[25-28] and for isomerizing systems; they are typically interpreted as twisted or partially isomerized ground-state populations.[25] The decay of the GSI in NpR6012g4 is multi-phasic on an apparent 10-ps time scale (Figs. 3B and 4B), with full decay occurring by 50 ps (Fig. 4C, green).

The discrepancy between the amplitude of the dump-induced depletion of P_r* (immediately after dumping) and the amplitude of the Lumi-R depletion (long after dumping) is significant. For example, the ESA signal at 470 nm exhibits ~21 % initial depletion (Fig. 3A), while the Lumi-R depletion at 6.3 ns is only ~11 % (Figs. 3 & 4). As further indicated by the overlap between the inverted and magnified (x7.5) ΔΔOD signal and the PP spectrum (Fig. 4D), this suggests that some of the dump-induced GSI can produce Lumi-R. The standard models used to interpret primary initiation photodynamics of isomerizing systems such as photoreceptor proteins instead predict a one-to-one correlation between excited-state depletion and photoproduct depletion (scaled by Φ).[12,13]

To demonstrate that the discrepancy between dump-induced depletion of P_r* and decreased Lumi-R yield is not a spectral or temporal artifact, a range of different probe wavelengths and times was investigated (Fig. 5). Since the ESA band from 440 to 525 nm (Fig. 1B) is a clean measure of P_r* population, it was used to estimate the dump-induced depletion. The ESA signal in the wavelength range of 440 to 525 nm was averaged at time points from 2.6 to 100 ps in Figure 5B (black circles). Similarly, the time-averaged ESA signal (from 2.6 to 100 ps) shown in Figure 5D (black circles) reveals that the ~21 % depletion extends to all wavelengths of the ESA. In contrast, the Lumi-R population (green circles) is depleted by a distinctly smaller amplitude of ~11 %. These results demonstrate that Lumi-R is forming from a species which was de-excited by the dump pulse, implying that Lumi-R need not be directly generated from P_r* on the excited-state potential energy surface.

An alternative explanation for the depletion discrepancy is that the dump pulse excites transitions other than the SE ($S_1 \rightarrow S_0$) to skew the comparison of the two depletions. The three possible transitions that can be pumped by the dump pulse are: P_r ($S_0 \rightarrow S_1$), Lumi-R ($S_0 \rightarrow S_1$), and P_r* ($S_1 \rightarrow S_n$). The first possibility can be excluded based on examination of the overlap of the dump laser spectrum with the ground-state spectra of P_r (Fig. 2A); furthermore no dynamics are observed in the DP signals other than the previously discussed artifacts (Fig. S1). The second possibility (exciting Lumi-R) is excluded, because the spectral overlap between Lumi-R and the dump-pulse is also negligible (Fig. 2, magenta curve) and because no significant population of Lumi-R has been generated at the 2-ps dump time (Fig. S4C).[16]

Excluding the third possibility of repumping of P_r* into one or more higher-lying states[22,29] requires more effort. Repumping P_r* may decrease the Lumi-R product yield by initiating higher-energy photochemistry (e.g., ionization) separate from the isomerization reaction on the lower excited-state energy surface. For this mechanism to be efficient, the 740-nm pulse must be resonant with an ESA ($S_1 \rightarrow S_n$); however, this is inconsistent with the PP signals (Fig. 2B), which show no clearly resolved (positive) ESA at the 740-nm dump wavelength. Only a strong SE band is resolved at 740-nm and at 2 ps. Furthermore, the fluorescence

spectrum (Fig. 2A, red curve)[30] tracks the same spectral trend as the SE, supporting resonance of the dump pulse with only the SE band. Moreover, the P_r* population is depleted by the dump pulse at 21 % and stays depleted at that level to 100 ps (Fig. 5B). Assuming that there is a higher lying excited-state population, the S_1 state would be expected to repopulate at least partially as population trickled down the excited-state manifold;[22] this is not observed in the PDP signals. Finally, for the P_r* repumping mechanism to be responsible for the depletion discrepancy (Fig.5), at least 50 % of the initial P_r* depletion must originate from repumping (assuming 100 % loss), with the rest originating from dumping. This would require the PP signal around the SE band to be near-zero, which is not the case here (Fig.4A and B, > 670 nm). Hence, for all of these reasons, the observed depletion of P_r* (and Lumi-R) is exclusively attributed to the dumping ($S_1 \rightarrow S_0$) of the excited-state P_r* population to form a non-equilibrated ground-state population.

Hence, the discrepancy between the depletion of P_r* and Lumi-R is also a dump-dependent effect that must result from a reactive GSI. The similar (albeit not identical) spectral features of the GSI and Lumi-R suggest that GSI adopts a twisted structure that has failed either to isomerize fully or to decay back to the ground state. The GSI decay kinetics are resolved in the 597-nm signals (Fig. 3B) with an apparent 10-ps lifetime. A fraction of GSI population must convert to Lumi-R on the *ground-state surface* to explain the discrepancy between the P_r* and Lumi-R depletions.

To quantify this, a previously proposed model constructed to interpret the PP signals alone[16] was extended to include dumping in the PDP data (Figs. 6A and S4).[31] The original model postulated multiple coexisting ground-state sub-populations (i.e., inhomogeneity) to describe the non-exponential PP kinetics. Only two out of three ground-state populations are productive for Lumi-R formation with an overall Φ of 32 %; the fastest 4.6-ps excited-state decay does not form Lumi-R.[16] Our dump-extended model posits that the GSI populations formed after dumping are connected to both productive excited-state intermediates (ESI 2 and ESI 3) and generate Lumi-R (30-ps time constant) or decay back in P_r (15 ps). The kinetics of this are resolved in the 10-ps decay PDP signals (Fig. 3B). As expected, the GSI spectrum (i.e., the Species Associated Difference Spectra or SADS[31]) exhibits a red-shifted absorption band (Fig. S4B), that is similar to normalized 2.6-ps transient spectrum (Fig. 4A).

This model successfully simulates both the PP and PDP signals (Fig. 3) and the dump-induced depletion properties (Fig. 5B and D), unlike analogous spectral models that exclude either GSI populations or their evolution to Lumi-R (Fig. S5 to S12). The calculated percent change based on the new target model (Fig. 6A) is in excellent agreement with the data (Fig. 5, solid lines). Thus, this analysis supports *second-chance* formation of Lumi-R from a novel GSI of NpR6012g4.

Moreover, additional parameters obtained from PDP data provide further constraints and amendment that confirm a Lumi-R quantum yield of 40 % (Fig. S4C). This is the highest Z → E Lumi-R quantum yield observed in any bilin-based sensor and is significantly higher than all known red/far red canonical phytochromes. This increased efficiency arises due to the NpR6012g4 ground-state dynamics, which provide a second pathway for generating Lumi-R (Fig. 6B). The existence of a productive GSI lying between P_r and Lumi-R on the ground-state reaction coordinate provides further support for a step-wise isomerization mechanism, in contrast to concerted mechanisms such as hula-twist[34] or bicycle-pedal[35] that do not require extensive cavity space for isomerization. Atomic resolution structural data of phytochrome systems show a less tightly packed cavity for D-ring in comparison to other rings, further supporting step-wise isomerization mechanism.[36-37]

The excited-state timescales of NpR6012g4 are similar to those of the cyanobacterial red/far-red phytochrome Cph1. However, in NpR6012g4, Lumi-R is not formed from the excited-state population with the fastest decay,[16] while Cph1 demonstrates rapid productive evolution of the structurally sensitive hydrogen-out-of-plane (HOOP) mode of the methine bridge between C and D ring.[38] Kennis and co-workers studied the PP signals of other bacterial phytochromes, observing nonproductive fast exited-state decay like that of NpR6012g4; this behavior was ascribed to D-ring twisting that increased tension within hydrogen-bond networks, some of which break for full isomerization with a low Φ (6-13 %).[13]

The exact nature of the twisted GSIs is to be studied further. It will be necessary to perform vibration-sensitive PDP experiments to describe these initiation dynamics at the molecular level. PDP approaches are necessary because of the inverted timescales, in which fast GSI evolution is masked by slower ESI evolution. It will also be interesting to see whether such a second-chance initiation mechanism is observed in other red/green CBCRs. The results we have obtained demonstrate the utility of the PDP experiment and reveal a new paradigm for photosensory proteins: the *second-chance* initiation mechanism as a important mechanism of generating high Φ.

Supplementary Material

Refer to Web version on PubMed Central for supplementary material.

Acknowledgments

We thank Lu Zhao for help with data collection. This work was supported by grants from the Chemical Sciences, Geosciences, and Biosciences Division, Office of Basic Energy Sciences, Office of Science, United States Department of Energy (DOE DE-FG02-09ER16117) to both J.C.L. and D.S.L. and the National Institutes of Health (GM068552) to J.C.L.

References

1. Rockwell NC, Su YS, Lagarias JC. Annual Review of Plant Biology. 2006; 57:837.
2. Auldridge ME, Forest KT. Critical Reviews in Biochemistry and Molecular Biology. 2011; 46:67. [PubMed: 21250783]
3. Franklin KA, Quail PH. Journal of Experimental Botany. 2010; 61:11. [PubMed: 19815685]
4. Ikeuchi M, Ishizuka T. Photochemical & Photobiological Sciences. 2008; 7:1159. [PubMed: 18846279]
5. Rockwell NC, Lagarias JC. Chemphyschem. 2010; 11:1172. [PubMed: 20155775]
6. Rockwell NC, Martin SS, Feoktistova K, Lagarias JC. Proceedings of the National Academy of Sciences of the United States of America. 2011; 108:11854. [PubMed: 21712441]
7. Gambetta GA, Lagarias JC. Proceedings of the National Academy of Sciences of the United States of America. 2001; 98:10566. [PubMed: 11553807]
8. Zhang JA, Wu XJ, Wang ZB, Chen Y, Wang X, Zhou M, Scheer H, Zhao KH. Angewandte Chemie-International Edition. 2010; 49:5456.
9. Shu XK, Royant A, Lin MZ, Aguilera TA, Lev-Ram V, Steinbach PA, Tsien RY. Science. 2009; 324:804. [PubMed: 19423828]
10. Moeglich A, Moffat K. Photochemical & Photobiological Sciences. 2010; 9:1286. [PubMed: 20835487]
11. Toh KC, Stojkovic EA, van Stokkum IHM, Moffat K, Kennis JTM. Physical Chemistry Chemical Physics. 2011; 13:11985. [PubMed: 21611667]
12. Kelly JM, Lagarias JC. Biochemistry. 1985; 24:6003.
13. Toh KC, Stojkovic EA, van Stokkum IHM, Moffat K, Kennis JTM. Proceedings of the National Academy of Sciences of the United States of America. 2010; 107:9170. [PubMed: 20435909]

14. Kim JE, Tauber MJ, Mathies RA. Biochemistry. 2001; 40:13774. [PubMed: 11705366]
15. Vanbrederode ME, Gensch T, Hoff WD, Hellingwerf KJ, Braslavsky SE. Biophysical Journal. 1995; 68:1101. [PubMed: 7756529]
16. Kim PW, Freer LH, Rockwell NC, Martin SS, Lagarias JC, Larsen DS. Biochemistry. 2011 Submitted.
17. Wang Q, Schoenlein RW, Peteanu LA, Mathies RA, Shank CV. Science. 1994; 266:422. [PubMed: 7939680]
18. Visser HM, Kleima FJ, vanStokkum IHM, vanGrondelle R, vanAmerongen H. Chemical Physics. 1996; 210:297.
19. Connelly JP, Muller MG, Bassi R, Croce R, Holzwarth AR. Biochemistry. 1997; 36:281. [PubMed: 9003179]
20. Devanathan S, Pacheco A, Ujj L, Cusanovich M, Tollin G, Lin S, Woodbury N. Biophysical Journal. 1999; 77:1017. [PubMed: 10423446]
21. Larsen DS, Vengris M, van Stokkum IHM, van der Horst MA, Cordfunke RA, Hellingwerf KJ, van Grondelle R. Chemical Physics Letters. 2003; 369:563.
22. Larsen DS, Papagiannakis E, van Stokkum IHM, Vengris M, Kennis JTM, van Grondelle R. Chemical Physics Letters. 2003; 381:733.
23. Kennis JTM, Larsen DS, Ohta K, Facciotti MT, Glaeser RM, Fleming GR. Journal of Physical Chemistry B. 2002; 106:6067.
24. Lorenc M, Ziolek M, Naskrecki R, Karolczak J, Kubicki J, Maciejewski A. Applied Physics B-Lasers and Optics. 2002; 74:19.
25. Rupenyan A, van Stokkum IHM, Arents JC, van Grondelle R, Hellingwerf KJ, Groot ML. Journal of Physical Chemistry B. 2009; 113:16251.
26. Larsen DS, van Stokkum IHM, Vengris M, van der Horst MA, de Weerd FL, Hellingwerf KJ, van Grondelle R. Biophysical Journal. 2004; 87:1858. [PubMed: 15345564]
27. Kennis JTM, Larsen DS, van Stokkum IHM, Vengris M, van Thor JJ, van Grondelle R. Proceedings of the National Academy of Sciences of the United States of America. 2004; 101:17988. [PubMed: 15608070]
28. Gai F, McDonald JC, Anfinrud PA. Journal of the American Chemical Society. 1997; 119:6201.
29. Larsen DS, Vengris M, van Stokkum IHM, van der Horst MA, de Weerd FL, Hellingwerf KJ, van Grondelle R. Biophysical Journal. 2004; 86:2538. [PubMed: 15041690]
30. Fukushima Y, Iwaki M, Narikawa R, Ikeuchi M, Tomita Y, Itoh S. Biochemistry. 2011; 50:6328. [PubMed: 21714499]
31. van Stokkum IHM, Larsen DS, van Grondelle R. Biochimica Et Biophysica Acta-Bioenergetics. 2004; 1657:82.
32. Muller MG, Lindner I, Martin I, Gartner W, Holzwarth AR. Biophysical Journal. 2008; 94:4370. [PubMed: 18199671]
33. Holzwarth AR, Venuti E, Braslavsky SE, Schaffner K. Biochimica Et Biophysica Acta. 1992; 1140:59.
34. Liu RSH. Accounts of Chemical Research. 2001; 34:555. [PubMed: 11456473]
35. Warshel A. Nature. 1976; 260:679. [PubMed: 1264239]
36. Wagner JR, Brunzelle JS, Forest KT, Vierstra RD. Nature. 2005; 438:325. [PubMed: 16292304]
37. Rockwell NC, Lagarias JC. Plant Cell. 2006; 18:4. [PubMed: 16387836]
38. Dasgupta J, Frontiera RR, Taylor KC, Lagarias JC, Mathies RA. Proceedings of the National Academy of Sciences of the United States of America. 2009; 106:1784. [PubMed: 19179399]

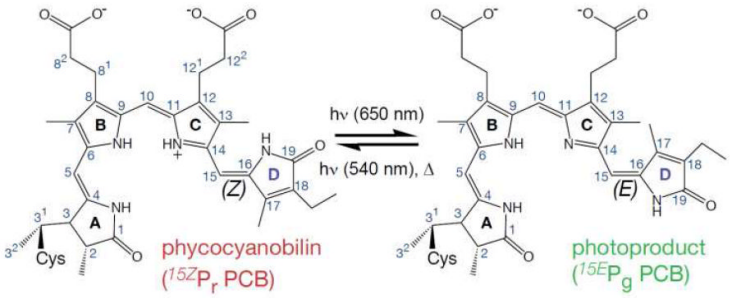

Figure 1.

Phycocyanobilin (PCB) chromophore and NpR6012g4's photochemistry. P_r is the dark-stable state with 15Z conformation, which isomerizes via C15,16-double bond to the higher energy 15E conformer P_g that can convert back to P_r photochemically or thermally.

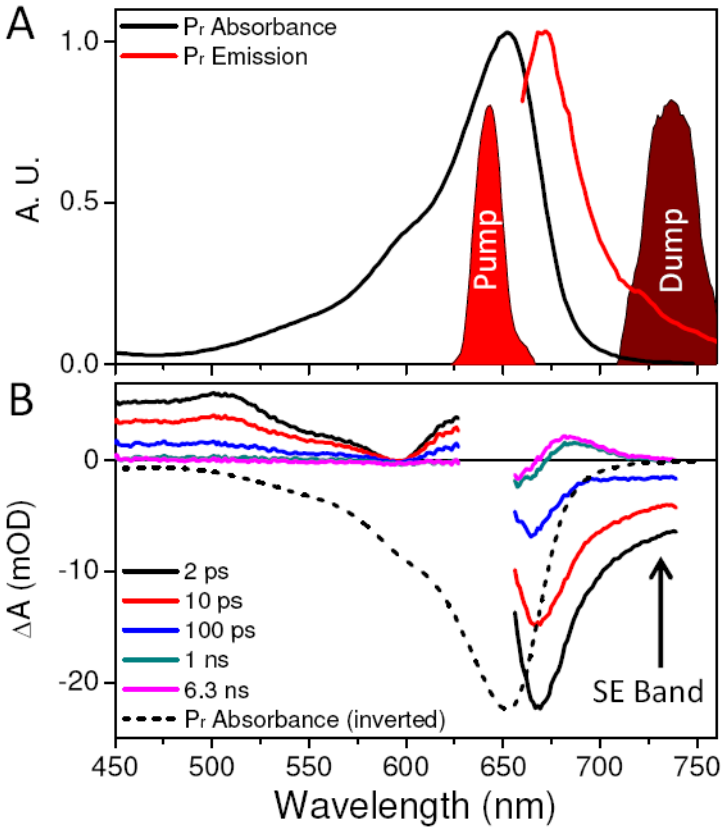

Figure 2.

(A) P_r ground-state spectrum (black line) and fluorescence emission band (red line) overlaid with spectra of pump (630 nm) and dump (740 nm) pulses. (B) Transient spectra of pump-probe data at selected probe times. The SE of the 2-ps transient spectrum overlaps the dump pulse spectrum. Inverted P_r absorption (black dashes) is shown for comparison.

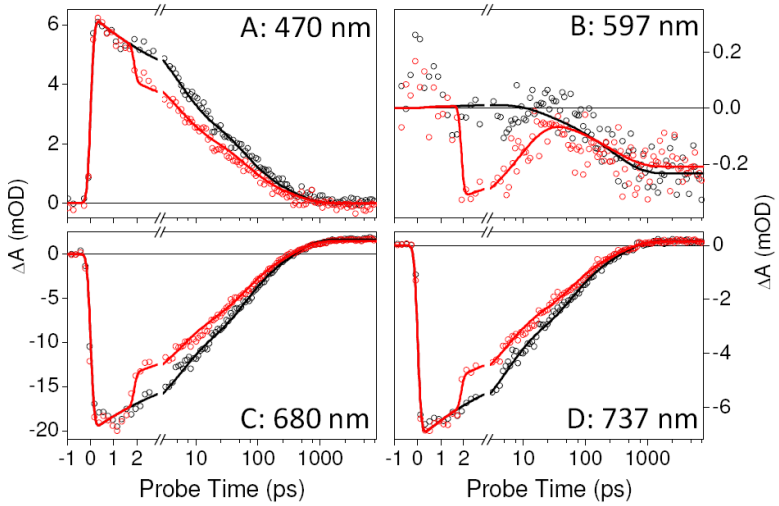

Figure 3.
Select kinetic traces of PP (black circle) and PDP (red circle) at wavelengths indicated. Both PP and PDP data are fitted with a kinetic model (solid lines) described in the Supporting Information (Fig. S4).

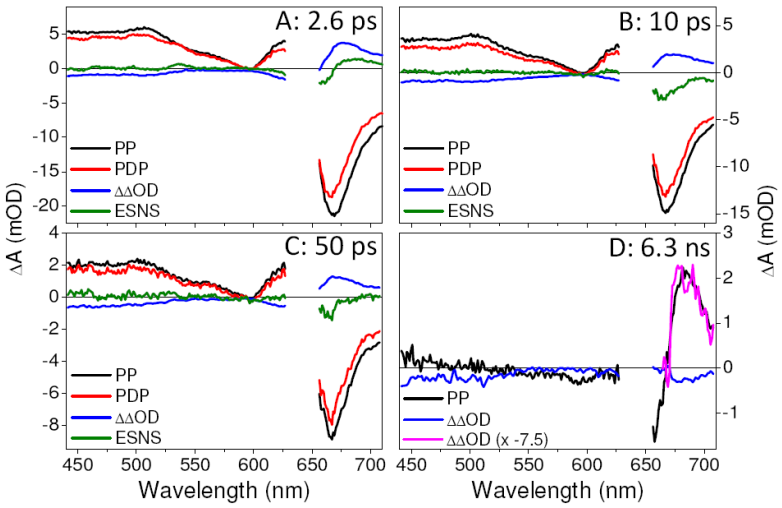

Figure 4.

Transient spectra of PP (black), PDP (red), and ΔΔOD (blue) at indicated probe times. The green line is ESNS, the difference spectrum between the PP and the PDP spectra normalized to the PP ESA band at 500 nm. At 2.6 ps, there is positive absorption red-shifted from P_r, indicating the formation of a GSI. The 6.3-ns spectrum shows dump-induced Lumi-R depletion indicated by decrease of the Lumi-R absorption amplitude. The 6.3-ns ΔΔOD is inverted, magnified (pink) and overlaid on the PP data.

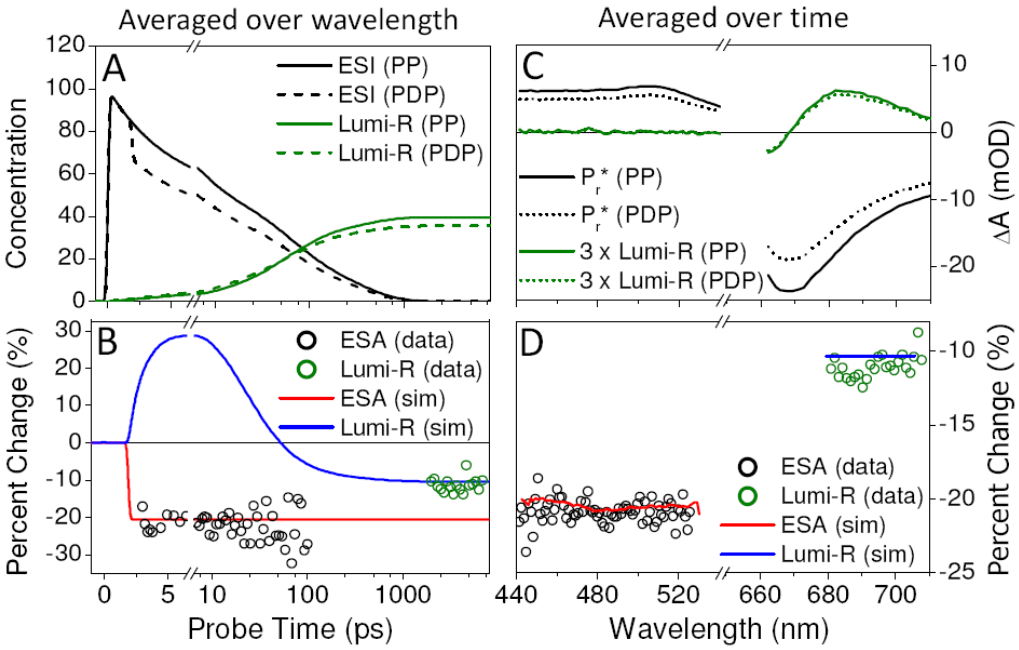

Figure 5.

Comparison of the average percent change of *initial* P_r* and *final* Lumi-R populations induced by the dump pulse. Percent change is calculated by (PP-PDP)/PP × 100 %. The simulation is based on the kinetic model in Figure 6A. Panels A and B are averaged over wavelengths: 440 to 525 nm and 680 to 705 nm for P_r* and Lumi-R, respectively. Panels C and D are averaged over time: 3 to 100 ps and 2 to 7 ns for P_r* and Lumi-R, respectively. (A) Simulated concentration profiles of P_r* (ESI1 + ESI2 + ESI3) and Lumi-R for both PP and PDP conditions. (B) Comparison between simulated P_r* and Lumi-R percent change (lines) and experimental percent change (circles) averaged over wavelengths. (C) PP and PDP spectra of P_r* and Lumi-R for reference. (D) Comparison between simulated (lines) and experimental (circles) P_r* and Lumi-R percent change averaged over time.

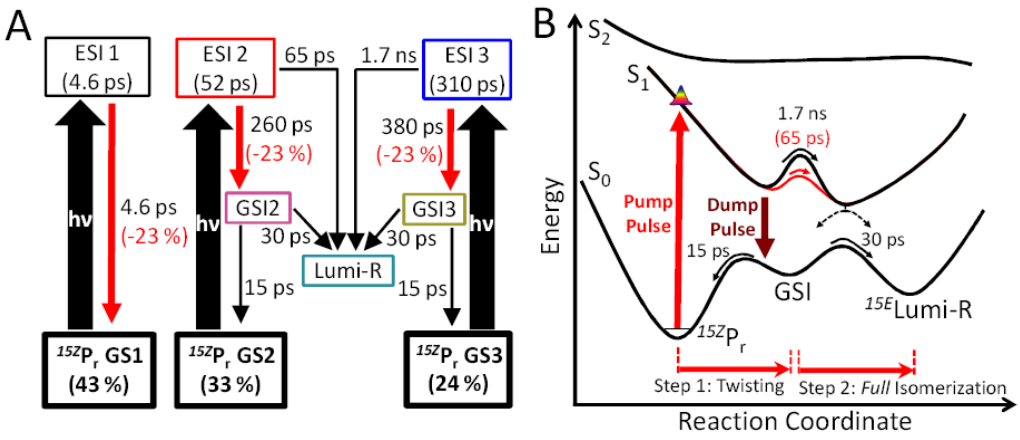

Figure 6.

(A) Kinetic model of NpR6012g4 forward reaction based on PDP data. (B) Potential Energy Surface[32-33] of the forward reaction based on target model in Panel A. Only the productive pathway from ESI 2 (potential barrier and time constant in red on S_1 potential surface) and ESI 3 (all black)are described here.